A Simple Analysis Showing the Limits of Coarse Particle Flotation

J. B. Dankwah[1], R. K. Asamoah[2], M. Zanin[1] and W. Skinner[1]
[1]ARC Centre of Excellence for Enabling Eco-Beneficiation of Minerals, University of South Australia, UniSA STEM, Future Industries Institute, Mawson Lakes, South Australia 5095
[2]University of South Australia, UniSA STEM, Future Industries Institute, Mawson Lakes, South Australia 5095

Dankwah J.B., Asamoah R.K, Zanin M., and Skinner, W. (2022), "A Simple Analysis Showing the Limits of Coarse Particle Flotation", *Proceedings of 7th UMaT Biennial International Mining and Mineral Conference*, Tarkwa, Ghana, pp. 1-7

Abstract

In this work, we investigate potential limitations to coarse particle flotation due to the finiteness of bubble surface area and the need for a bubble-particle aggregate to have a lower density than the fluid medium for particle collection to be possible. We derived a simple mathematical model which assumes perfect collection efficiency (E = 1) and spherical particles. The model was simulated using a python script and the data obtained is as presented in this paper. Our results indicate that the maximum number of particles attached to a bubble surface depends not only on bubble size but also on fluid density and particle density, especially at extreme coarse sizes. However, this does not necessarily lead to higher particle loads per bubble in terms of mass. Whiles increased fluid density generally increases the maximum bubble load, this increase is not monotonous and may not influence performance within some size ranges.

Keywords: Bubble size, Particle size, Coarse particle flotation, Density

1 Introduction

Flotation is one of the most used concentration processes in the metallurgy industry. It is easily adaptable to most ores and cost-effective. With current trends in decreasing ore grades, increasing energy costs, and the complexity of ores, processing materials at coarser sizes to minimize costs has become a critical objective of the processing industry (Calvo et al., 2016, Maron et al., 2019, Asamoah et al., 2021).

Coarse particle flotation provides an avenue for minimizing costs and therefore, enhancing the profitability of the processing companies that rely on it. Literature on the subject breaks down the particle collection process into three stages i.e., collision, attachment, and stability (or detachment) (Tao, 2005, De F. Gontijo et al., 2007). In the collision stage, the feed particle moves within a distance short enough for attachment forces between the bubble and the particle to start interacting. If the particle is hydrophobic enough, and the contact time between the particle and bubble is long enough, the particle attaches to the bubble surface forming an aggregate. The stability of the formed bubble-particle aggregate is determined by its likelihood to remain attached. The process of the particle separating from the bubble is known as detachment. The likelihood of a particle being collected (E) is expressed as a probability of these subprocesses (Ralston et al., 1999):

$$E = E_c \cdot E_a \cdot E_s$$

Where E_c is the probability of collision, E_a is the probability of attachment and E_s is the probability of stability.

The general assumption is that if E = 1, then a particle must be recovered under the given flotation conditions. Based on this, most flotation research is based on controlling one of these factors. In fine particle flotation, the goal is to enhance E_c which seems to be the limiting factor of the process while in coarse particle flotation, the goal is to enhance Es which seems to be the limiting factor (Jameson et al., 2007, Jameson, 2010, Kohmuench et al., 2018, Tao, 2005, De F. Gontijo et al., 2007). These

assumptions generally hold true with the literature showing that fine particle flotation performance is enhanced by controlling E_c and coarse particle performance is enhanced by controlling E_s (Jameson, 2010, Dankwah et al., 2022, Awatey et al., 2014, Kohmuench et al., 2018, Tao, 2005).

However, with flotation being a surface phenomenon and a physical process where the formed aggregate requires a density lower than that of the fluid to be collected, there may be inherent limits beyond which optimizing these sub-processes may prove futile. In this work, we show what these limits may be by relying on a mathematical model to answer the following questions:

1. What is the maximum number of particles that can attach to a bubble surface?
2. Is there an inherent maximum bubble load?
3. What is the influence of particle size on (1) and (2)?
4. What other factors may influence (1) and (2)?

2 Mathematical Model

2.1 Maximum number of particles attached to a bubble surface (C_{max})

Flotation is a surface phenomenon. The general model is that of a particle attached to a bubble surface as shown in Figure 1A. Assuming a bubble is a sphere, its surface area, A, can be defined as:

$$A_b = 4\pi R^2$$

Where R is the bubble radius.

Assuming an equivalent surface area of a square, Figure 1B shows the optimal arrangement of particles in such an area. From this, the portion of bubble surface area used by each particle is the square of its diameter. Therefore, the maximum number of particles, C_{max}, that can be attached to a bubble of surface area, A_b, is given as:

$$C_{max} = \frac{A_b}{(2r)^2}$$

Where r is the particle radius.

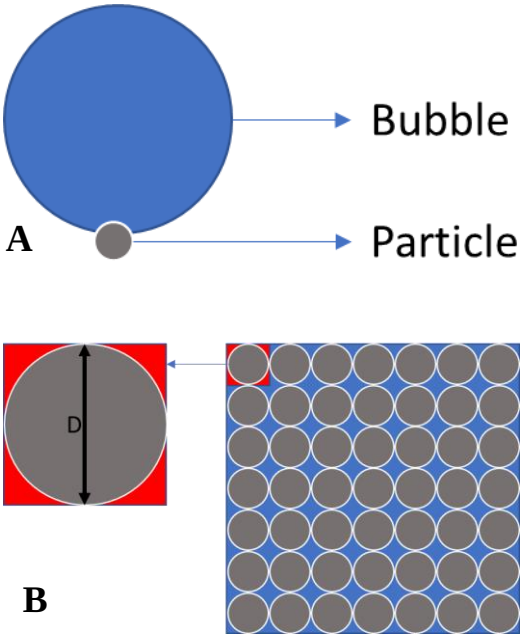

Figure 1 (A) Illustration of general bubble-particle aggregate model (B) Illustration of particle arrangement on a bubble of a given surface area equivalent to a square

2.2 Bubble load resulting from particles attached to a bubble surface

The bubble load resulting from C_{max} is given by:

$$L_{max} = C_{max} * \rho * V_p$$

Where ρ is the particle density and V_p is the particle volume which is assumed in this case to be the volume of a sphere.

2.3 Density of a bubble-particle aggregate

The density of the resulting bubble-particle aggregate can be calculated as the total mass divided by the total volume:

$$\rho_{agg} = \frac{L_{max}+m_b}{(C_{max}*V_p)+V_b}$$

Where V_b is the bubble volume, which can also be calculated as a sphere, and m_b is the bubble mass which is assumed to be zero in this case given its low density.

2.4 Simulation in Python

A python script was written to simulate the derived equations. The logic was to first calculate the total possible C_{max} irrespective of the aggregate density.

Once this was obtained, the number of particles was iteratively reduced until the aggregate density fell below the fluid density. In some cases, C_{max} was 0 indicating that particle collection at the given parameters was physically impossible. The results from the simulation were in the form of CSV files with data on particle size (incremented by 50 from 100 microns to 3000 microns), C_{max}, $L_{max,}$ and the flotation status (true if the aggregate density is lower than the fluid density and false if otherwise).

3 Results and Discussions

3.1 Effect of feed particle size on the maximum number of particles attached to a bubble surface (C_{max})

Figure 2 shows the relationship between particle size and the maximum number of particles that can attach to a bubble surface (C_{max}). C_{max} is an exponential decay function of particle size. As the particle size increases, the possible number of particle attachments quickly approaches zero. This is mainly because of the square increase in bubble surface area used due to particle size for smaller particles, and the tendency of the aggregate density to exceed the fluid density for coarser particles. For a bubble size of 1 mm, only one particle in the size range of 700 –1000 µm can be attached. Any higher and the aggregate density exceeds the fluid density, deeming the aggregate uncollectable. For a bubble size of 2 mm, this size range increases to 1400 – 2000 µm whiles for a 3 mm bubble, the size range is 2100 – 3000 µm. Bubble size influences the number of particles that can be attached by providing a higher surface area and increasing the load threshold for identical aggregate densities.

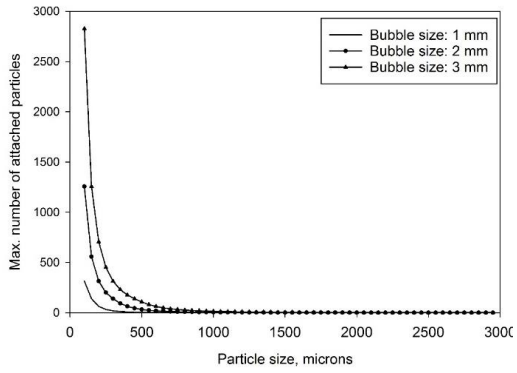

Figure 2 Relationship between the maximum number of particles attached to a bubble surface and feed particle size.

3.2 Effect of particle size on maximum bubble load (L_{max})

While smaller particle sizes allow more particles to attach to a bubble surface, this does not necessarily translate to enhanced bubble load. Figure 3 shows the relationship between feed particle size and the maximum possible bubble load (L_{max}). Bubble loads for relatively finer particles seem to be limited by the finiteness of the bubble surface area. The surface area is exhausted before peak load is attained therefore leading to inefficient loading. The bubble load then stabilizes for some size range before it begins to swing. This 'volatility' is due to the change in C_{max} as the size range increases. For some size ranges, C_{max} remains constant and bubble load increases across the size range as the particle size increases. However, when this size range is exceeded, the drop in C_{max} causes a noticeable drop in load, and then increases as the particle size increases in this new size range. These drops in load due to C_{max} become more obvious as the overall particle size increases.

From Figure 3, the maximum bubble load is attained as particle size increases to the exact point at which the aggregate density exceeds that of the fluid density. The relationship is influenced by bubble size following its influence on C_{max} but the general trend is consistent.

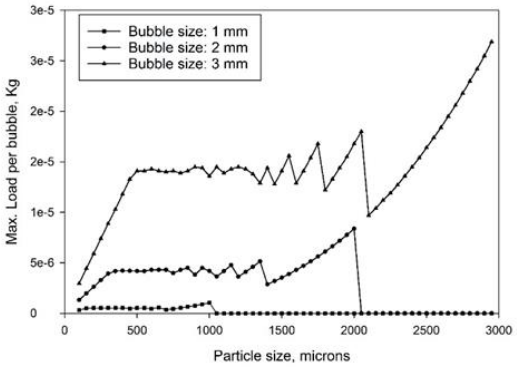

Figure 3 Maximum load per bubble as a function of feed particle size and bubble size.

3.3 Effect of particle size on bubble load optimization

For a bubble of a given size to be fully optimized in flotation, its resulting aggregate density must be as close to the fluid density as possible. This means its particle carrying capacity is fully used. Figure 4 shows the effect of feed particle size on the

resulting aggregate density. Smaller feed particles underutilize bubble carrying capacity. This follows from the bubble surface limitation explained above leading to lower bubble loads than would be optimal. Beyond this size range, there is a size range within which bubble optimization is consistent. This size range depends on the bubble size used (150 – 400 µm for a 1 mm bubble, 300 – 700 µm for a 2 mm bubble, and 500 – 1250 µm for a 3 mm bubble). This size range increases as bubble size increases but beyond that, another optimum seems to be attained at a feed particle size right before aggregate density exceeds fluid density.

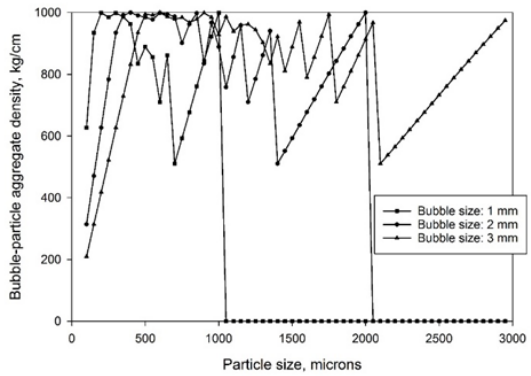

Figure 4 Maximum bubble-particle aggregate density as a function of particle size and bubble size

3.4 Effect of particle density on C_{max} and L_{max}

Figure 5A below shows the relationship between C_{max} and feed particle size for a 2 mm bubble and a fluid SG of 1. While bubble surface area is a potential limitation of C_{max} at relatively finer particle sizes, particle density may also be a limiting factor on C_{max}. Data generated from this simulation shows that C_{max} starts to vary after 200 µm for the feed particle sizes considered, with C_{max} for particle density of 3 dropping to 170 at 250 µm from an initial of 201 for the particle densities of 1 and 2. This eventually leads to a limitation on the upper floatable particle size with a particle density of 1 being 3000 µm, particle density of 2 being 2000 µm and particle density of 3 being 1550 µm. Given that denser particles require fewer numbers to match the load on the bubble, this observation is expected and agrees with the literature on the subject. However, the key observation is that within a size range (< 250 µm in this case), there may be no noticeable drop in flotation performance for denser particles.

Figure 5B shows the relationship between L_{max} and feed particle size because of the change in C_{max} due to particle density. The limitation of bubble surface area at finer particle sizes is made up for by denser particles bearing higher masses for equivalent surface areas. This can be seen from the initial point of the graph as the particle sg of 3 attains a higher L_{max} before the sgs of 2 and 1 catch up around 400 µm and 800 µm respectively. However, given the huge drop in load of denser particles for little drops in C_{max}, bubble load is unable to attain a maximum at coarser particle sizes. The less-dense sg of 1 allows subtle increases in bubble load for each increase in particle size without the aggregate density exceeding the fluid density. This leads to better bubble load utilization at coarser sizes.

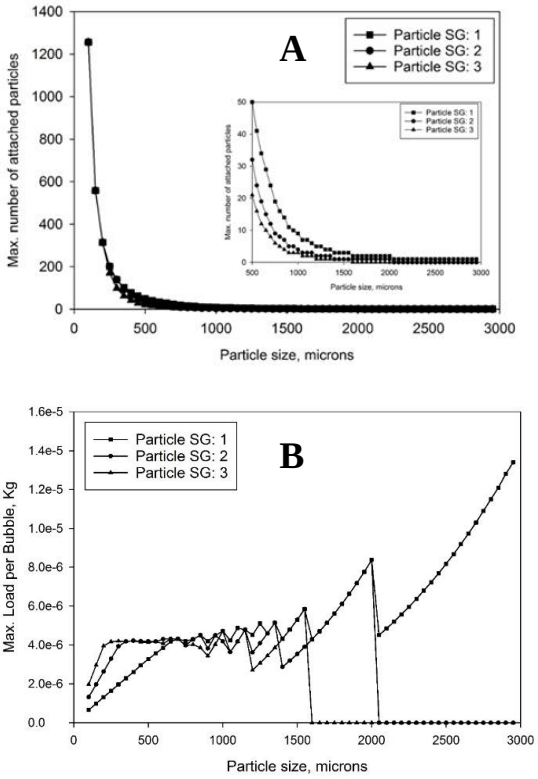

Figure 5 Influence of particle SG on (A) the relationship between C_{max} and feed particle size and (B) the relationship between L_{max} and feed particle size

3.5 Effect of particle density on bubble optimization

The resulting aggregate densities from Figure 5 are shown in Figure 6. Continuing the discussion from

3.4, the bubble's capacity is fully used for denser particles at relatively finer sizes. Given that higher particle density allows more load per bubble surface used, the aggregate density peaks at the fluid sg as soon as the size range within which C_{max} is limited is exceeded. However, as particle size increases further, this same phenomenon leads to huge swings in aggregate density that affect the optimization of the bubble's capacity. Particle density also dictates the maximum floatable particle size agreeing with the literature on the subject (Shi and Fornasiero, 2009).

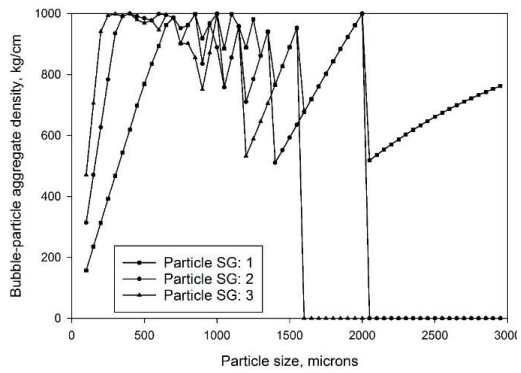

Figure 6 Influence of particle SG on resulting bubble-particle aggregate density as a function of feed particle size

3.6 Effect of Fluid Density on C_{max}, L_{max}, and Bubble Density Optimization

We showed in a previous publication that controlling fluid density could be a way to enhance coarse particle flotation performance (Dankwah et al., 2022). This was mainly through a lowering of the particle weight in fluid and a consequent limitation of detachment forces. Data from our model shows that as far as the upper limit of recovery is concerned, there are some size ranges within which this strategy works, and others where controlling fluid density does not affect performance. Figure 7A shows the relationship between C_{max} and feed particle size at varying fluid sgs whiles Figure 7B shows the relationship between L_{max} and feed particle size at varying fluid sgs. Fluid sg serves as the maximum possible sg beyond which an aggregate cannot be recovered. From our data, increasing fluid sg to any level at a feed size range < 350 µm shows no influence on C_{max}. This is because the bubble surface is already fully utilized and is the limitation to further performance, not aggregate density. Between 350 and 450 µm, an increase from a fluid sg of 1 to 1.5 increases C_{max} but a further increase to 2 does not affect C_{max}. Above this size range, increasing fluid sg shows enhanced C_{max} and L_{max} consequently until 1700 µm where a major increase from an sg of 1 to 2 is required for a change in C_{max} and L_{max} to be seen. From there, C_{max} at a fluid sg of 1.5 and 2 remain the same until the upper floatable size for the sg of 1.5 is reached. This is mostly a balancing act between aggregate density and fluid density.

The effect of fluid sg on C_{max} and L_{max} continues into bubble load optimization. Figure 7C shows the effect of fluid sg on the relationship between particle size and aggregate density. Given that increasing fluid sg is increasing the upper bound of the aggregate density, the trends in the graph are mostly similar aside from the vertical and horizontal shifts due to the increase in fluid sg.

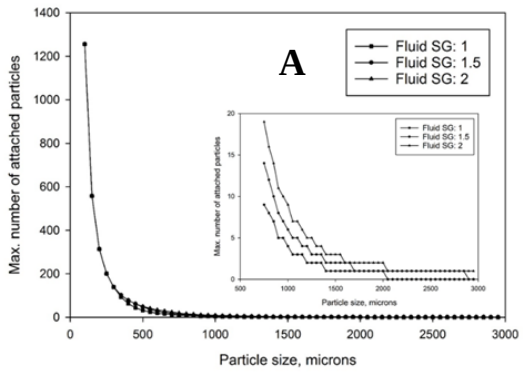

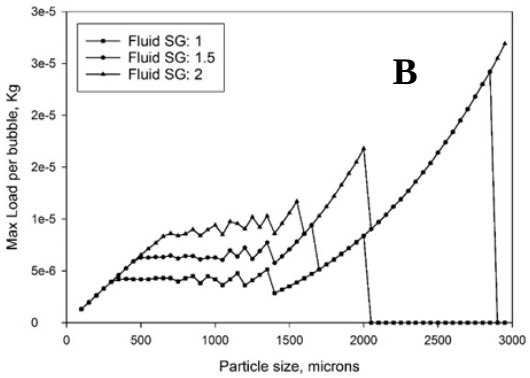

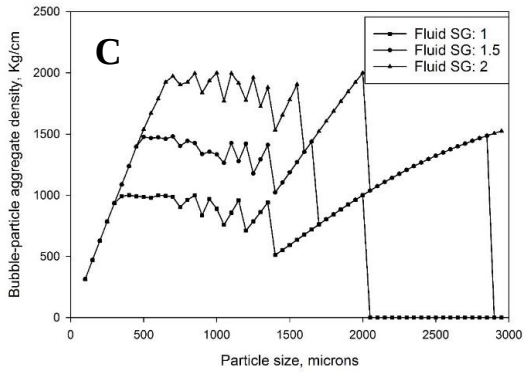

Figure 7 Influence of fluid sg on the relationship between (A) C_{max} and feed particle size (B) L_{max} and feed particle size (C) Bubble-particle aggregate density and feed particle size

4 Conclusions

1. The maximum number of particles attached to a bubble surface is an exponential decay function of feed particle size, but this relationship does not necessarily affect the maximum bubble load adversely.

2. At finer sizes, bubble load is limited by the finiteness of the bubble surface area whiles at coarser sizes, it is limited by the tendency for the aggregate density to exceed that of the fluid density.

3. Controlling fluid density provides an avenue to enhance coarse particle flotation performance. However, this may only be optimum over some size ranges.

4. Numerous physical factors such as bubble size, particle density, and fluid density may place an inherent limit on the maximum floatable particle size even when the efficiency of collection is maximized (E = 1).

Acknowledgements

The authors acknowledge the funding support from the Australian Research Council for the ARC Centre of Excellence for Enabling Eco-Efficient Beneficiation of Minerals, grant number CE200100009.

References

Asamoah, R. K., Baawuah, E., Greet, C. and Skinner, W. 2021. Characterisation of metal debris in grinding and flotation circuits. *Minerals Engineering,* 171**,** 107074.

Awatey, B., Thanasekaran, H., Kohmuench, J. N., Skinner, W. and Zanin, M. 2014. Critical contact angle for coarse sphalerite flotation in a fluidised-bed separator vs. a mechanically agitated cell. *Minerals Engineering,* 60**,** 51-59.

Calvo, G., Mudd, G., Valero, A. and Valero, A. 2016. Decreasing ore grades in global metallic mining: A theoretical issue or a global reality? *Resources,* 5**,** 36.

Dankwah, J., Asamoah, R., Zanin, M. and Skinner, W. 2022. Dense liquid flotation: Can coarse particle flotation performance be enhanced by controlling fluid density? *Minerals Engineering,* 180**,** 107513.

De F. Gontijo, C., Fornasiero, D. and Ralston, J. 2007. The limits of fine and coarse particle flotation. *The Canadian Journal of Chemical Engineering,* 85**,** 739-747.

Jameson, G. J. 2010. New directions in flotation machine design. *Minerals Engineering,* 23**,** 835-841.

Jameson, G. J., Nguyen, A. V. and Ata, S. 2007. The flotation of fine and coarse particles. *Froth Flotation: A Century of Innovation.* Denver, CO, USA SME, 329 - 351.

Kohmuench, J., Mankosa, M., Thanasekaran, H. and Hobert, A. 2018. Improving coarse particle flotation using the HydroFloat™(raising the trunk of the elephant curve). *Minerals Engineering,* 121**,** 137-145.

Maron, R., Sepulveda, J., Jordens, A., O'Keefe, C. and Walqui, H. 2019. Coarser Grinding: Economic Benefits and Enabling Technologies. Proceedings of MINEXCELLENCE 2019, 4th International Seminar on Operational Excellence in Mining, Santiago, Chile. 1 - 10.

Ralston, J., Fornasiero, D. and Hayes, R. 1999. Bubble–particle attachment and detachment in flotation. *International Journal of Mineral Processing,* 56**,** 133-164.

Shi, Y. and Fornasiero, D. 2009. Effects of particle size and density, and turbulence on flotation recovery. *Engineering Our Future: Are We up to the Challenge?: 27-30 September 2009, Burswood Entertainment Complex***,** 528.

Tao, D. 2005. Role of bubble size in flotation of coarse and fine particles—a review. *Separation science and technology,* 39**,** 741-760.

Author

James B. Dankwah is a Ph.D. candidate at the Future Industries Institute (FII), University of South Australia, Australia. James has a BSc (Hons) in Minerals

Engineering from the University of Mines and Technology, Tarkwa, Ghana. His research interest includes Coarse Particle Flotation.

Richmond K. Asamoah is a research fellow of the minerals and resources engineering at the Future Industries Institute (University of South Australia), having over eight years in-depth knowledge of and hands-on experience in mineral characterisation and extractive metallurgy in tandem with molecular chemistry and interfacial science. He has specialised diagnostic and prognostic skills in laboratory operations for industry-specific methodical investigations, and simulation and modelling of process flowsheets.

Max Zanin is Associate Research Professor in Mineral Processing. He holds a BEng (Hons) in Mineral Processing Engineering (University of Trieste) and a PhD in Geo-engineering (University of Cagliari). His research interest specialises in Mineral processing: froth flotation, physical separation, Urban Mining and solid waste treatment, Sustainable use of resources and optimization of processes. He is a member of the Australasian Institute of Mining & Metallurgy (AusIMM), and of the Australian Colloid and Interface Society (ACIS). Max is currently part of the CSIRO Sustainable E-waste Processing initiative.

William Skinner is a Research Professor and Strand Leader - Minerals and Resource Engineering, Future Industries Institute (FII), University of South Australia, Australia. Areas of his research interest include Flotation (pulp and surface chemistry); Leaching (including heap); Physical Separation and other nit Operations (including surface effects); Surface Chemical Control in Grinding/Milling; Mineral formation-Processing Relationships; Bulk Property-Surface Reaction Relationships in Processing Contexts (oxidation, activation, dissolution and molecular adsorption); Agglomeration Chemistry; Impact of Water Chemistry on Processing, Mineral Sands; Synthetic Rutile and Pigment Processing, etc.